Measurement of polarization transfer in Møller scattering of relativistic electrons

Michał Drągowski * and Jacek Ciborowski
University of Warsaw, Faculty of Physics, Pasteura 5, 02-093 Warszawa, Poland

Marek Adamus
National Centre for Nuclear Research, Świerk, Sołtana 7, 05-400 Otwock, Poland

Joachim Enders and Yuliya Fritzsche
Technische Universität Darmstadt, Fachbereich Physik, Institut für Kernphysik, Schlossgartenstr. 9, 64289 Darmstadt, Germany

Marco Dehn and Valery Tioukine
Johannes Gutenberg–Universität Mainz, Institut für Kernphysik, Johann-Joachim-Becher-Weg 45, 55128 Mainz, Germany

(Received 30 June 2021; accepted 5 October 2021; published 29 November 2021)

A dedicated Mott polarimeter was designed to study the final spin state in Møller scattering of transversely polarized electron beams in the relativistic energy range. The polarization transfer was measured for two incident-beam polarization orientations with respect to the Møller scattering plane, at 3 MeV incident-beam energy. The results are found to be in agreement with the predictions of relativistic quantum mechanics. Estimates for the measurement of quantum spin correlations in Møller scattering, based on a simultaneous determination of the spin projections for both electrons in the final state, are also presented.

DOI: 10.1103/PhysRevD.104.092011

I. INTRODUCTION

The first relativistic description of electron–electron scattering has been given by Møller [1]. Since then, this process has been extensively studied in several important experiments. This included, in particular, the measurement of the cross section asymmetry in Møller scattering of longitudinally polarized electron beams, which can be used to test the parity violation in electroweak interactions [2]. The resulting precision of the weak mixing angle measurement is comparable to the best results from colliders [3]. Another application is the Møller polarimetry method, which has become the standard tool for beam polarization measurement in high-energy spin physics [4–6], complementary to the Mott polarimetry method used at low energies [7].

Even though Møller scattering has been studied in great detail over its almost 100 year history, it still offers unexplored research opportunities. Considerable effort has been put into theoretical research focused on a particular case of the Einstein–Podolsky–Rosen correlations [8] involving massive particles. While the quantum spin correlations and the violation of Bell–type inequalities [9] have been measured for protons originating from low-energy nuclear reactions [10–12], no experimental studies of this kind have been performed with massive particles in the relativistic regime.

The quantum spin correlation function for a two-electron final state is defined by four probabilities of obtaining given outcomes in spin-projection measurements performed on both entangled particles. The quantum spin correlation function and the corresponding probabilities for electrons in the final state of Møller scattering have recently been calculated in a special case of polarized electron beam scattering off an unpolarized target [13], as well as the scattering of two polarized electrons [14], assuming the Mott polarimetry technique for spin projection measurement. These calculations show that the studies of the final spin state in Møller scattering of polarized electron beams open new research perspectives and become a unique tool for testing relativistic spin observables and quantum entanglement in the range of relativistic energies. A measurement of this kind was first proposed in [15].

The main experimental challenge of such a measurement is related to the low interaction probability leading to a signal-to-background ratio many orders of magnitude lower than in the case of a standard polarization

*mdragowski@fuw.edu.pl

measurement performed on a beam. The signal events are extremely rare due to the low combined probability of Møller and two coincident Mott scattering processes, of the order of 10^{-15} per incident beam electron with kinetic energy of 3 MeV. Additionally, the Mott polarimeter has to operate, in contrast to the conventional applications, on a divergent stream of secondary Møller electrons, which further increases the background contribution.

The primary aim of this work was to directly measure the polarization transfer in Møller scattering (the ratio of the transverse polarization vector component length of the electron in the final state to the incoming-beam polarization); it is, to our knowledge, the first such measurement. The average polarization of the electrons in the final state of near-symmetric Møller scattering is measured using Mott polarimetry. The results are compared to the predictions of relativistic quantum mechanics [14].

The study presented in this work is a prerequisite for measuring spin correlations, in that it is focused at measuring the spin projection of one final-state Møller electron. The additional aims of the study were, therefore, to test a standard Mott polarimeter as a prototype tool for a correlation experiment and to obtain guidelines for the design of a double-polarimeter device.

II. MØLLER SCATTERING

The initial state of two electrons (before the scattering) can be described by a product of density matrices, as the states of colliding electrons are prepared separately. In contrast, the outgoing electrons may be entangled in consequence of the scattering, so neither of them is found in a well-defined polarization state separately. Therefore, it is, in general, impossible to assign polarization vectors to the electrons after the scattering, because only their joint polarization state is well defined by the density matrix [13]. Nevertheless, one can use the reduced density matrices of the final state electrons to assign mean polarization vectors to both of them [14].

When a 100% polarized beam is scattered off an unpolarized stationary electron, both electrons in the final state are partially polarized. In the symmetric scattering configuration (90° scattering angle in the center-of-mass frame, corresponding to the laboratory scattering angle $\theta = 26.75°$ for an incident electron with kinetic energy of 3 MeV),[1] both outgoing electrons have the same polarization due to the indistinguishability of the particles. However, in an asymmetric configuration, in particular, for very small scattering angles, the electron with higher energy inherits the majority of the incoming electron polarization. This is illustrated in Fig. 1 for a transversely polarized 3 MeV beam. The transverse polarization of

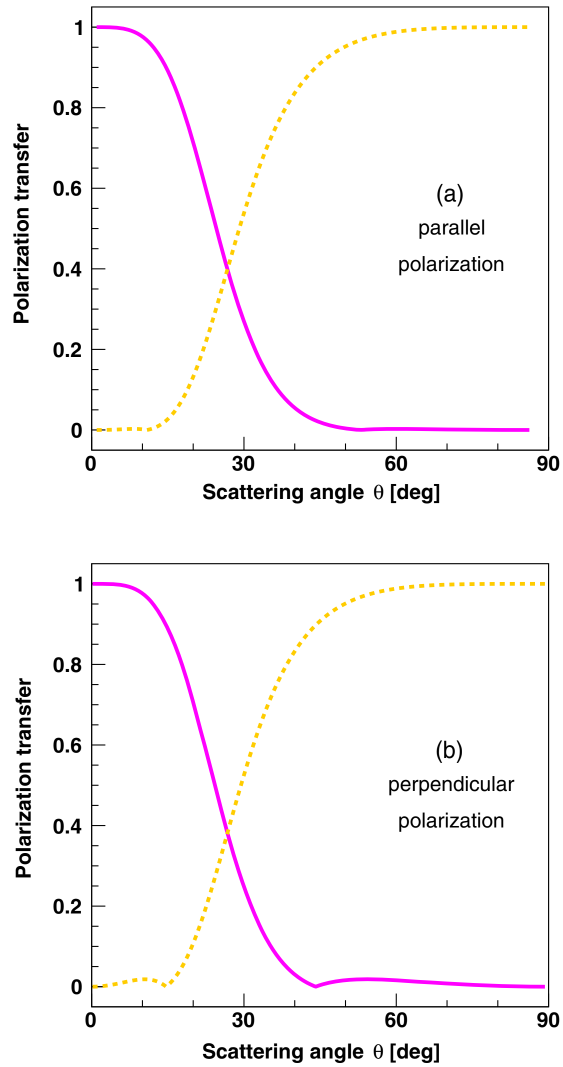

FIG. 1. Polarization transfer from a transversely polarized 3 MeV beam electron to the secondary Møller electrons, (a) beam polarization in the Møller scattering plane, (b) beam polarization perpendicular to the Møller scattering plane. The polarization transfer (length of the transverse polarization vector component divided by the initial beam polarization) dependence on the scattering angle θ (measured in the laboratory frame of reference) is plotted with the solid line. The corresponding polarization of the second electron is plotted with a dashed line. Equal polarization sharing occurs for the symmetric scattering configuration ($\theta = 26.75°$ for incident electrons with 3 MeV kinetic energy, which corresponds to 90° in the center-of-mass frame).

symmetric Møller electrons is equal to approximately 0.399 of the beam polarization if the beam polarization vector lies in the Møller scattering plane and approximately 0.382 if the beam polarization is perpendicular to the Møller scattering plane.

III. EXPERIMENTAL SETUP

The study of the polarization transfer in Møller scattering of a polarized electron beam amounts to measuring the

[1]Throughout the paper, all kinematic quantities refer to the values in the laboratory frame of reference unless explicitly stated otherwise.

electron spin projection on a given direction in space; Mott polarimetry is a standard method in the MeV energy range. However, the signal-to-background ratio in the case of a Mott measurement performed on particles originating from a reaction process is many orders of magnitude lower than in the case of a typical Mott polarimeter operating on a primary beam. Additionally, the measurement is challenging in the range of relativistic energies due to the low cross sections for the combined double-scattering process.

The method is based on measuring the azimuthal asymmetry, arising from the spin–orbit interaction, in scattering of a polarized electron beam off thin targets made of heavy elements. The differential cross section for Mott scattering off a single atom is given by [16]

$$\left(\frac{d\sigma}{d\Omega}\right)_{\mathrm{Mott}} = \left(\frac{d\sigma}{d\Omega}\right)_{0}(1 + S(E,\theta)\vec{P}\cdot\vec{n}), \tag{1}$$

where the cross section $(d\sigma/d\Omega)_0$ describes the scattering of unpolarized electrons, $S(E,\theta)$ is the Sherman function describing the analyzing power of Mott scattering, E is the kinetic energy of the beam, θ is the polar scattering angle, $\vec{P}$ is the electron polarization vector and $\vec{n}$ is the unit vector normal to the scattering plane, $\vec{n} = \vec{p}\times\vec{p}'/|\vec{p}\times\vec{p}'|$, where $\vec{p}$ and $\vec{p}'$ denote the momenta of the incoming and scattered electron, respectively.

The measurement can be done with a single detector by reversing the beam polarization direction; the asymmetry A is then defined as

$$A = \frac{N^{\uparrow} - N^{\downarrow}}{N^{\uparrow} + N^{\downarrow}}, \tag{2}$$

where $N^{\uparrow}$ and $N^{\downarrow}$ are the count rates of electrons Mott-scattered off the target for opposite beam polarizations. If the measurement is performed using two detectors, denoted L and R, placed symmetrically with respect to the beam axis, at a given angle θ, the combined asymmetry can be calculated using [17]

$$A = \frac{1-\sqrt{Q}}{1+\sqrt{Q}}, \tag{3a}$$

with

$$Q = \frac{N_L^{\uparrow}N_R^{\downarrow}}{N_L^{\downarrow}N_R^{\uparrow}}. \tag{3b}$$

Thanks to the fact that the measurement was performed reversing the polarization direction at 1 s intervals, the detector efficiencies cancel out in the above equations and do not contribute to the uncertainty.

The component of the polarization vector perpendicular to the scattering plane is related to the asymmetry as follows:

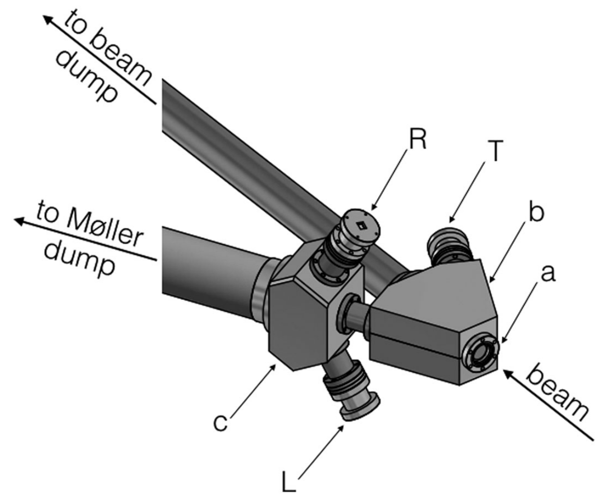

FIG. 2. Drawing of the experimental setup in configuration A (vertical Mott scattering plane, see text for details): a, Møller (Be) target; b, Møller scattering chamber; c, Mott scattering chamber; T, tagging counter; L and R, detectors in the Mott polarimeter. The shielding and the full length of the dump pipes are not shown.

$$\vec{P}\cdot\vec{n} = \frac{A}{S_{\mathrm{eff}}(E,\theta)}, \tag{4}$$

where the theoretical value of the Sherman function S, cf. Eq. (1), appropriate for scattering off a single atom, was replaced with its effective value S_{eff}, in which multiple interactions of the electron in the target material are taken into account.

The theoretical Sherman function can be calculated numerically, for example, with the widely used ELSEPA package [18]. The calculation of the effective Sherman function requires a full Monte Carlo simulation with particle tracking and polarization transfer, in particular, when thick targets are used, resulting in a large contribution of multiple scattering. The simulation was performed with the Geant4 toolkit [19] supplied with a dedicated Mott scattering model [20].

The experimental setup is shown in Fig. 2. In the present experiment, Møller scattering was realized by scattering a polarized electron beam off atomic electrons in a target made of beryllium, 100 μm thick. The electrons scattered off the beryllium target passed through two pipes (below called legs), positioned at an angle of 26.75° with respect to the primary beam direction, corresponding to the symmetric Møller scattering at 3 MeV beam energy. One leg was equipped with a Mott polarimeter. The other leg was terminated with a detector pointing directly at the beryllium target, below referred to as the tagging counter. Collimators placed in the legs accepted Møller scattering events close to the symmetric kinematical configuration only (in the range $26.75° \pm 1.5°$, corresponding to a solid angle of 8.6×10^{-3} sr). Beam electrons passing through the

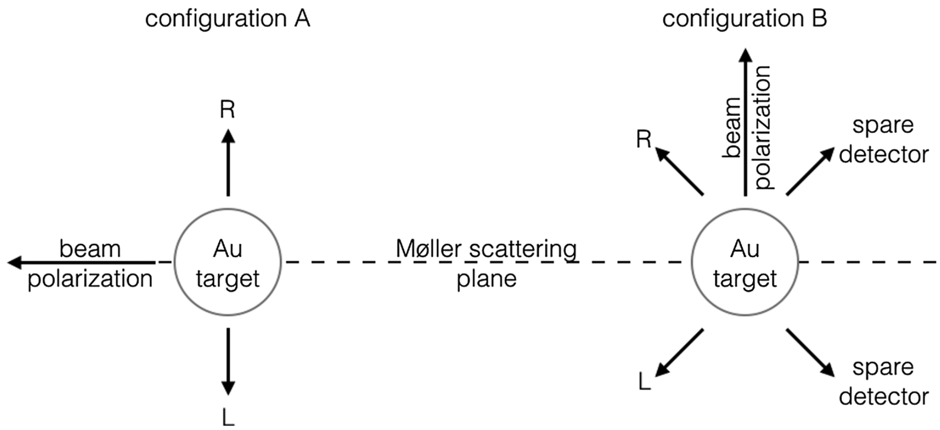

FIG. 3. Schematic illustration of both experimental configurations (cross section in the gold-target plane, perpendicular to the direction of the Møller-electrons stream); L and R denote the locations of the detectors in the Mott polarimeter.

beryllium target (scattered at small angles) were absorbed in a beam-dump material (graphite and aluminum) approximately 2 m downstream.

The polarization of one of the electrons in the final state of Møller scattering, as well as the polarization of beam electrons (Mott-scattered off the beryllium target), could be measured in the Mott polarimeter. Collimators in the Mott polarimeter restricted the measurement to electrons backscattered off a 9.9 μm thick gold target at an angle of $120° \pm 5°$ (corresponding to the solid angle of 9.5×10^{-2} sr).

An aluminum frame holding the gold target was mounted in one slot of an aluminum ladder, which could be moved remotely between two positions. The other slot contained an empty target frame identical to that holding the gold foil. The position of the ladder was changed periodically, allowing us to measure the empty-target background, which was then subtracted from the data acquired with the gold foil.

Electrons passing through the gold target (scattered at small angles) were absorbed in a Møller dump material (plastic). The inside walls of the Mott scattering chamber, as well as the pipes leading to the dumps, were covered with graphite in order to reduce backscattering. In order to eliminate scattering off air atoms, a vacuum of approximately 10^{-7} mbar was maintained inside the setup. The surroundings of the Mott polarimeter, in particular, the whole space between the detectors and the beam pipe, were packed with lead bricks to shield against the external background.

The measurements were performed in two configurations of the Mott polarimeter, corresponding to different beam polarization orientations: (A) horizontal beam polarization (in the Møller scattering plane) and vertical Mott scattering plane and (B) vertical beam polarization (perpendicular to the Møller scattering plane) and Mott scattering plane at an angle of 45° to the Møller scattering plane. Both configurations are shown schematically in Fig. 3. The asymmetry reaches its maximum when the polarization vector is perpendicular to the Mott scattering plane, cf. Eq. (4). Thus, the best resolution would be achieved in configuration B with a horizontal Mott scattering plane, but this was not possible in the present polarimeter design for geometrical reasons.

In configuration B, owing to the 45° angle between the Mott and Møller scattering planes, and the symmetry with respect to the polarization vector direction, there are four equivalent directions of measurement in the Mott polarimeter. The background originating from electrons scattered off the beryllium target towards the beam pipe and other parts of the setup resulted in significantly different background conditions in detectors placed close to and far from the beam axis, despite thick shielding. The additional symmetry allowed us to place the detectors in the pair of locations subject to the lowest level of background, more distant from the beam pipe.

The scattered electrons were detected using scintillation counters. A silicon photomultiplier sensor was used to detect the scintillation light. Short response time and pulse width ensured precise timing required for a coincidence trigger of the tagging and one of the polarimeter detectors, used to record Møller scattering events. The pulse height analysis allowed for an approximate energy calibration, sufficient to distinguish the electrons originating from Møller scattering from scattered beam electrons, whose energy is on average twice as high.

IV. DATA ACQUISITION AND ANALYSIS

A. Data acquisition

The measurements were performed with a 3 MeV polarized electron beam from the injector linac of Mainzer Mikrotron (MAMI) [21]. The experimental conditions were as follows: beam energy (3.0000 ± 0.0003) MeV, beam spot diameter of the order of 1 mm, beam angular dispersion 1.5 mrad.

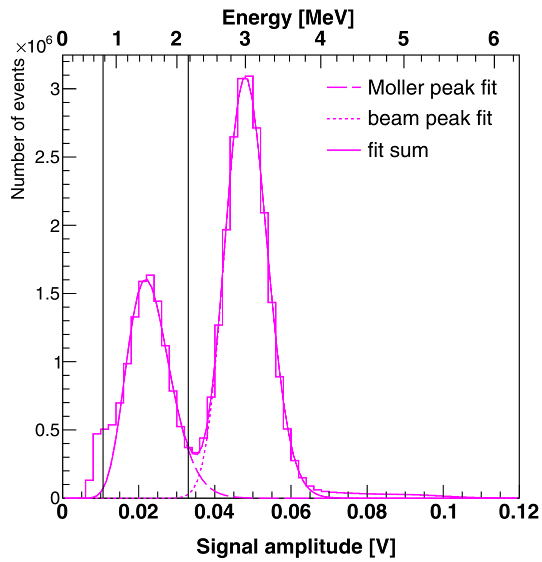

FIG. 4. Signal amplitude spectrum in the tagging counter pointing directly at the beryllium target. The higher peak consists of Mott-scattered beam electrons, and the lower peak of Møller electrons. The black vertical lines indicate the cuts applied to select the Møller scattering events.

The polarization of the beam (Mott-scattered off the beryllium target), as well as the mean polarization of electrons in the final state of Møller scattering, was measured. The beam polarization measurement was repeated every day; this way the polarization obtained after combining data from all runs should correspond to the mean value over the whole data taking period of the Møller scattering experiment. Additionally, half of the runs were taken with a half-wave plate in the laser system of the polarized electron source yielding a 180° flip of the electron spin orientation, allowing us to reduce part of the systematic errors arising from a possible polarization-correlated asymmetry of electronics. Furthermore, in half of the runs, the Mott target was replaced with an empty target frame in order to record the background, which was then subtracted from the data collected with the target.

The tagging counter recorded Mott-scattered beam electrons (of approximately 3 MeV energy) as well as Møller electrons (of 1.5 MeV on average). Together with one of the detectors in the polarimeter, it produced a coincidence trigger used to record symmetric Møller scattering events. It also allowed us to infer the energy spectrum of particles reaching the Mott polarimeter. A typical raw signal amplitude spectrum is shown in Fig. 4, and an approximate energy calibration is also shown for reference. The peak at higher energies corresponds to the beam electrons Mott-scattered off the beryllium target, while the peak at lower energies to the Møller electrons.

Data from the polarimeter were collected with two different triggers: (i) Møller trigger (coincidence of any of the polarimeter detectors with the tagging counter) and (ii) beam trigger (detectors in the polarimeter read out without coincidence). Data acquisition took place in configuration A for 86 hours with Møller and 8 hours with beam trigger and in configuration B for 114 hours with Møller and 14 hours with beam trigger.

B. Dead time correction

The signals from the detectors were digitized with a switched capacitor array circuit [22]. When the trigger condition was met, the data acquisition was stopped until the readout was finished. As a result, a dead time of about 2 ms was introduced, when no events could be recorded. The dead time observed in the experiment also included the latency introduced by the computer which read the data from the digitizer board and stored them to a hard drive.

The effective correction, taking into account both sources of dead time, was determined from the distribution of time between consecutive events recorded during the experiment, which was fitted with an exponential function. The recorded number of events was multiplied by the ratio of the fitted (dead time free) event rate to the event rate recorded in the experiment.

Since the dead time correction depends on the count rate, which was different for the data acquired with opposite beam polarizations, as well as for the data acquired with the gold target and with an empty target frame, it has to be properly taken into account when calculating the asymmetry. The numbers of recorded events were corrected, and the histograms were reweighed, on a run-by-run basis.

The dead time correction to the count rate was between 50% and 70% with the beam trigger (count rate approximately 190 evt/s) and approximately 50% with the Møller trigger (count rate approximately 150 evt/s). The dead time correction to the asymmetry was approximately +10% of the measured asymmetry value with the beam trigger and approximately +2% with the Møller trigger. For the dead time contribution to the uncertainty, see Sec. V A.

C. Beam polarization

Data acquired with the beam trigger was used to determine the incident electron-beam polarization. A typical spectrum recorded in the Mott polarimeter (i.e., after beam Mott scattering both off the beryllium and gold targets), after dead time correction, before and after background (empty target frame runs) subtraction, is shown in Fig. 5 for two opposite beam polarizations. The asymmetry arising due to the beam polarization is clearly visible.

A significant fraction of remaining internal, target-related background events, including Møller electrons, is also visible in the low-energy part of the spectrum shown in Fig. 5(b). The asymmetries were obtained by counting events in the right half of the beam peak, where the signal-to-background ratio is sufficiently high that subtraction of this remaining background is not necessary. According to an exponential fit to the background tail, the fraction of

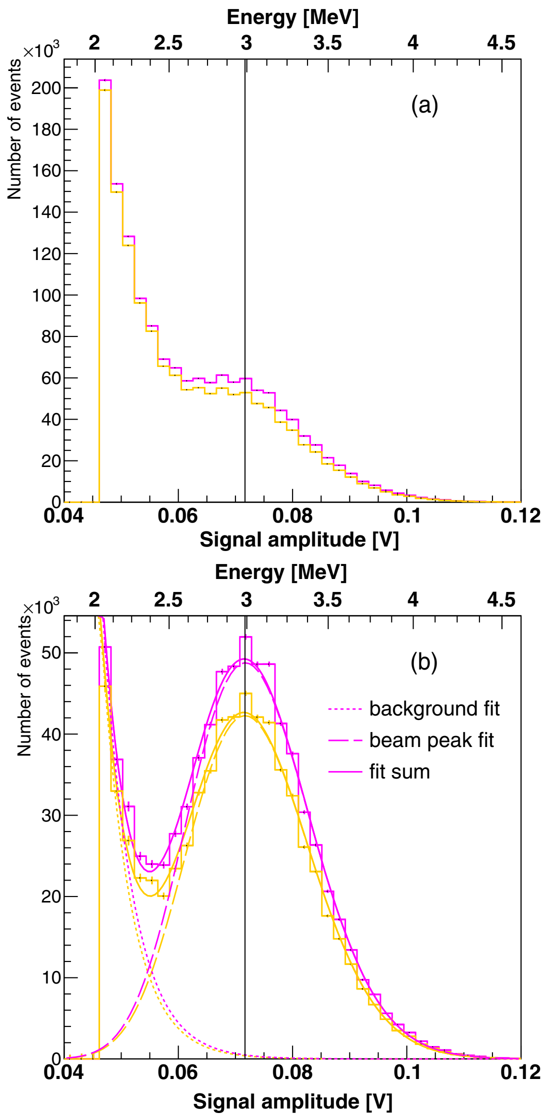

FIG. 5. Typical signal amplitude spectrum, recorded in the polarimeter with the beam trigger, before (a) and after (b) offline background subtraction. Histograms for opposite beam polarizations are plotted with different colors. The peak corresponds to beam electrons Mott-scattered off the beryllium and gold targets. The black vertical line indicates the low-amplitude cut used to calculate the asymmetry.

remaining background events in the data sample is approximately 1%.

D. Møller electrons polarization

In order to record the Møller electrons in the polarimeter, a coincidence trigger of the tagging and one of the polarimeter detectors was used. As in the beam polarization measurement, the number of events recorded with an empty target frame was subtracted from the number of events recorded with the gold target foil.

In addition to the shielding mentioned in Sec. III, a further reduction of background was achieved by event selection based on restricting values of two variables: (1) energy (signal amplitude) in the tagging detector and (2) arrival-time difference of the polarimeter and tagging detector signals. The time distribution is shown in Fig. 6; a Gaussian peak, about 2 ns wide, corresponding to the coincidences of Møller electrons, is clearly visible on top of a uniform background.

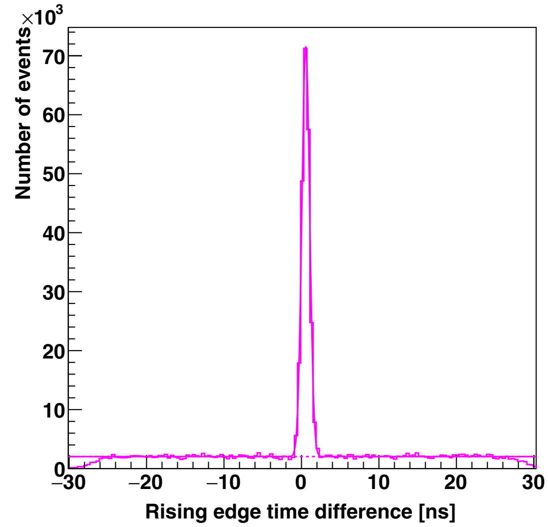

FIG. 6. Histogram of the time distance between the rising edge position in the polarimeter and the tagging detector, after empty-target background subtraction, for events with signal amplitude within $\pm 2\sigma$ of the Møller peak. The distribution is fitted with a sum of a constant (background) and a Gaussian (signal), shown with a solid line. The background interpolation under the signal peak is marked with a dashed line.

The signal amplitude spectrum recorded in one of the polarimeter detectors with the Møller trigger, after dead time correction, is shown at the subsequent stages of the analysis procedure in Fig. 7. The data sample recorded with the Møller trigger is dominated by background events, which has to be corrected for using data collected with an empty target frame. After background subtraction, two peaks become clearly visible. The one around 1.5 MeV corresponds to Møller electrons, which give the coincidence signal, while the smaller peak around 3 MeV results from false coincidences of Mott-scattered beam electrons. The final asymmetries were obtained by counting events in the Møller peak with $\pm 2\sigma$ amplitude cuts marked in Fig. 7.

V. MEASUREMENT UNCERTAINTIES

A. Statistical uncertainty

In case of the beam polarization measurement, the statistical uncertainty reflects mainly the number of recorded signal events. This is, however, not the case for Møller electrons. In this case, the signal-to-background ratio ranges from 1 to approximately 0.05 in different parts of the Møller peak, so in general, the statistical uncertainty

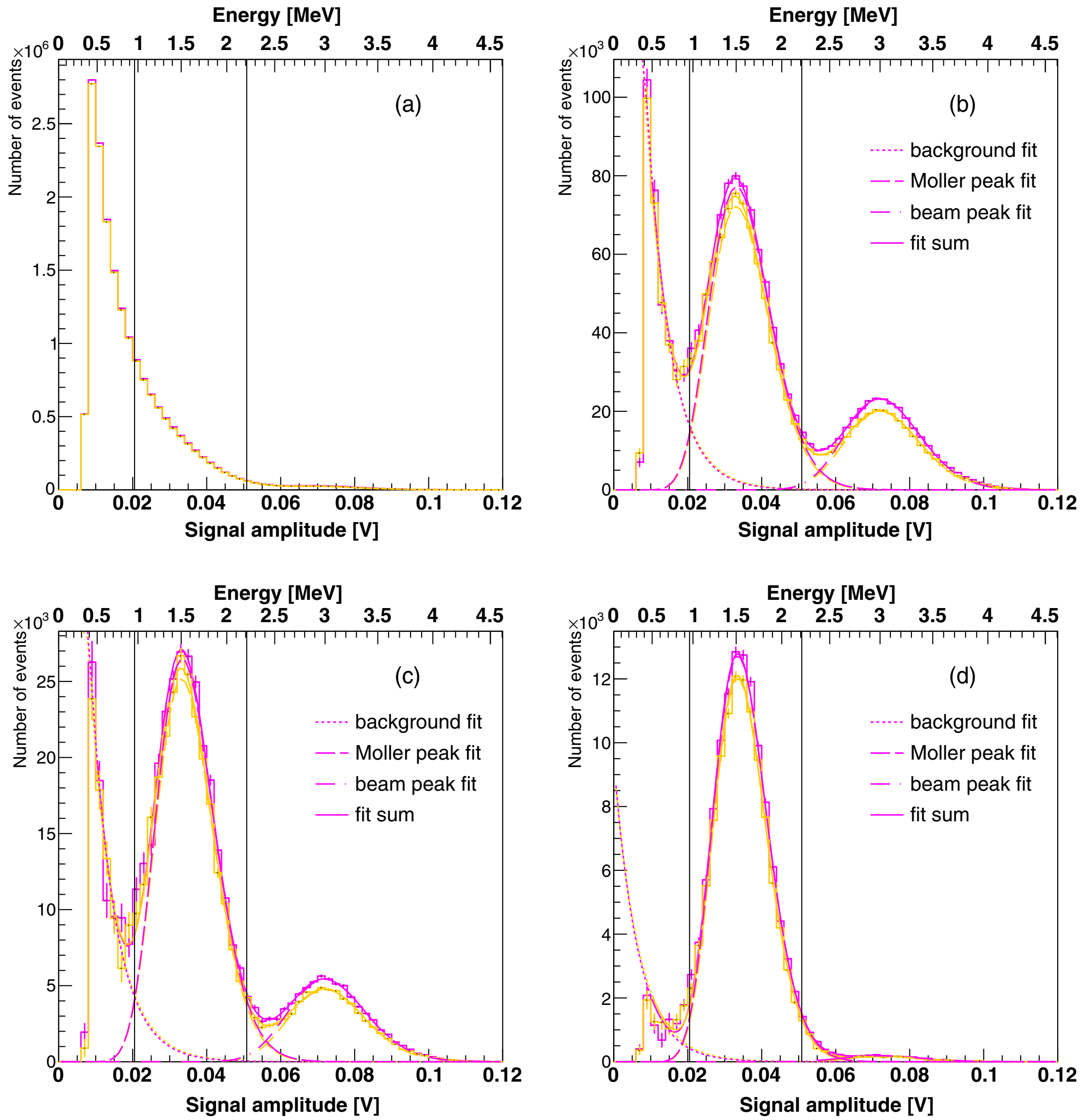

FIG. 7. Typical signal amplitude spectrum, recorded in the polarimeter with the Møller (coincidence) trigger, before offline background subtraction (a), after background subtraction (b), after background subtraction and energy cuts in the tagging detector (c) and after background subtraction and energy and timing selections (d). Histograms for opposite beam polarizations are plotted with different colors. The peak around 1.5 MeV corresponds to Møller electrons backscattered off the gold target and the peak at higher energies to doubly Mott-scattered beam electrons (false coincidences). The black vertical lines mark the part of the spectrum used to calculate the asymmetry.

follows mostly from the number of registered background events. Since the background spectrum is in agreement with an exponential distribution, the higher-energy part of the peak is subject to a much lower uncertainty than the low-energy tail of the Møller peak.

The dead time correction is as well subject to a significant statistical uncertainty, since it is based on fits to the experimental time distributions, which was also included in the total statistical uncertainty. The contribution of the dead time correction to the asymmetry uncertainty is approximately 0.0006 with the beam trigger and 0.0003 with the Møller trigger.

B. Analyzing power

In view of the lack of experimental data on the effective Sherman function under the conditions of this experiment, a dedicated Monte Carlo simulation [20] was used to optimize the parameters of the Mott polarimeter, including target thickness and scattering angle. The simulated values of the analyzing power, 0.0847 at 3 MeV and 0.0886 at 1.5 MeV, were then used for data analysis. The effective Sherman function at beam energy could be determined experimentally, from the measured asymmetry and the independently measured beam polarization. However, since the final result is the ratio of the polarizations before and after the scattering, it is advisable to use the values of the analyzing power obtained from the same method both at 1.5 and 3 MeV energies. This way the ratio is less sensitive to a possible systematic error of the Monte Carlo predictions, which partly cancel out.

The gold target thickness uncertainty was estimated at 10%. The effective Sherman function was calculated for the extreme values of 8.9 μm and 10.9 μm. This way the systematic uncertainties of the analyzing power related to the target thickness were estimated as ± 0.0014 at 3 MeV and ± 0.0026 at 1.5 MeV.

The Monte Carlo simulation was validated by comparing its predictions to the experimental values from a few different polarimeters operating at energies between 100 keV and 14 MeV. The systematic uncertainties of the Monte Carlo predictions were estimated by analyzing the differences between the simulations and the values measured with the MAMI Mott polarimeter for energies from 1 to 3.5 MeV and several target thicknesses [23]; the details will be presented elsewhere [24].

The total systematic uncertainties of the analyzing power, taking into account both effects, were estimated as ± 0.0034 at 3 MeV and ± 0.0063 at 1.5 MeV.

C. Dependence on applied cuts

The asymmetry was calculated for several values of the low-energy cuts applied to both Møller and beam spectra recorded in the polarimeter. The effective analyzing power was adjusted accordingly based on the Monte Carlo simulation results. The polarization uncertainty related to this effect was estimated from the range of polarization values obtained with different cuts as approximately ± 0.01.

Several timing cuts and energy cuts in the tagging detector were tested as well, and the values resulting in the lowest uncertainty were used, while no significant dependence of the result on these selections was observed.

D. Target-related background

The background events can be divided in two classes: (i) empty-target background, which can be removed by subtracting the data acquired with an empty target frame and (ii) target-related background remaining after the subtraction.

The latter class of events consists of the low-energy background, whose spectrum can be described approximately as exponential, as well as Mott-scattered beam electrons, with energy around 3 MeV. The asymmetry of the low-energy background is much smaller than that of the signal, while the asymmetry for the beam electrons is higher than for Møller electrons. Therefore, the former type of events could decrease and the latter increase the measured asymmetry.

For the data collected with the beam trigger, the number of target-related background events was estimated from the fits to the spectrum, which are also shown in Fig. 5(b). For the data collected with the Møller trigger, the number of such events passing the selection criteria was calculated by interpolating the time difference distribution between the polarimeter and tagging detector signals. This method, independent of the background energy distribution, relies on the assumption that the time distribution of background events (false coincidences) is uniform. The validity of this approach was verified by establishing an upper limit on the existence of an additional background peak on top of the uniform distribution using the data collected with an empty target frame. No additional contribution was found within the statistical uncertainty.

E. Beam current stability

Another factor, which could affect the asymmetry measurement, is the stability of the beam current. The data were acquired in four-run sequences: the target in—target out—target out—target in. If the beam current was stable or changing linearly with time, the above order would ensure that the average event rate is unbiased in the signal as well as the background (empty target frame) data. In the contrary case there would be a wrong amount of background subtracted from the raw data. The background runs taken with a higher (lower) current than the signal runs would result in an increased (decreased) asymmetry.

The data were corrected by assigning each run a weight equal to the ratio of the average event rate (signal or background) during the whole data taking period to the average event rate during this run; the weight variation was in the range $\pm 10\%$. The resulting asymmetry correction for the beam current instability is, however, negligible (order of 10^{-4}). The final asymmetry turns out to be insensitive to this effect as the random changes of the beam current average out to a large extent when data from all runs are combined.

F. Finite thickness of the Møller target

Møller scattering took place in a relatively thick target (100 μm), while the theoretical predictions refer to the scattering off an isolated electron. As a result of multiple scattering off atomic nuclei, the passage of electrons through the target material affects their state in two ways: it causes depolarization and alters the kinematics. The first effect was estimated with a Monte Carlo simulation taking into account the polarization transfer in Mott scattering; the depolarization in the passage of 3 MeV electrons through 100 μm of beryllium is negligible (below 0.1%) in the case of the electrons that are scattered at small angles. The kinematic effect of multiple scattering is more significant, as it leads to the broadening of the energy (or angular) range of accepted Møller scattering events. However, since the polarization transfer dependence on the scattering angle is approximately linear, and the analyzing power almost constant in the considered energy range, the effect on the experiment result was found negligible.

G. Beam position

The beam spot position with respect to the geometrical center of the beryllium target affects the kinematic range of events accepted by the collimators. This effect is particularly important if the beam is off center in the Møller scattering plane. In this case, due to the scattering geometry, the average energy of Møller electrons is different from the design value of 1.5 MeV. The upper limit on this energy difference was estimated with a Monte Carlo simulation as 0.04 MeV. The change of the polarization transfer corresponding to this energy variation was determined from the theoretical predictions and amounts to approximately ± 0.013.

H. Scattering off the collimators

If the beam was perfectly focused in the center of the beryllium target, it would be extremely unlikely that an electron outside of the nominal acceptance of the collimators scatters off the collimator surface and reaches the polarimeter. According to a Monte Carlo simulation, only about 0.1% of events recorded on the Mott target would fall into that category. However, taking into account the real beam spot diameter of approximately 1.5 mm and beam position uncertainty up to 1 mm, the simulated fraction of such events might be as high as 4.2% in the most pessimistic scenario. The systematic uncertainty related to this effect was estimated by assuming that the electrons scattered off the collimators are completely depolarized, which allowed us to calculate the upper limit on the asymmetry reduction. The upper limit on the contribution to the asymmetry is approximately -4.4% of the measured asymmetry value.

I. False asymmetries

The empty-target asymmetries with the beam trigger were found to be 0.0044 ± 0.0029 and 0.0188 ± 0.0057, in configurations A and B, respectively. The empty-target background might have a nonzero asymmetry due to the fact that there is a small but nonzero analyzing power in electron scattering off the aluminum target frame.

Thanks to higher statistics, the empty-target asymmetry can be measured with a much better precision in the energy range corresponding to Møller electrons. The asymmetry obtained with the Møller trigger was 0.0002 ± 0.0005 in configuration A. The single-counter asymmetry values were 0.0033 ± 0.0007 and 0.0037 ± 0.0008, which indicate that there was a small false asymmetry in the experimental setup that cancels out when when data from two detectors are combined. A small change of the beam position in the direction perpendicular to the beam polarization direction is the most likely explanation of the observed asymmetry with respect to the beam-polarization reversal.

In configuration B, the empty-target asymmetry with the Møller trigger was 0.0059 ± 0.0008, and the single-counter asymmetry values of 0.0060 ± 0.0010 and 0.0059 ± 0.0012 are in perfect agreement. The cancellation of false asymmetries might not take place in this configuration because the detectors were not placed opposite of each other. According to the Monte Carlo simulation, a 0.2 mm difference between the beam positions for opposite polarizations would produce an asymmetry in the intensity of background electrons scattered off the collimators of approximately 0.0063 (i.e., of the same order as the experimental value). The corresponding asymmetry calculated for all electrons recorded on the Mott target (most of which are not scattered off the collimators, cf. Sec. V H) would be, however, more than a factor of 5 lower. It is thus reasonable to assume that the false asymmetry in the signal data is approximately $1/5$ of the measured empty-target asymmetry, which was included in the systematic uncertainty for configuration B. Nevertheless, the contribution of this false asymmetry partly cancels out in the polarization ratio.

J. Radiative corrections

The magnitude of the radiative corrections to Mott scattering is expected to be increasing with energy [25] and might produce a significant contribution to the effective analyzing power with respect to the Monte Carlo-generated value. However, since the systematic uncertainty of the Monte Carlo predictions was estimated by comparing the simulated and measured values, this effect is already included in the uncertainty.

In the case of Møller scattering, the radiative corrections were estimated following the calculations of Tsai [26]. At 3 MeV, the correction to the cross section is below 1%; therefore, in our experimental conditions, this effect can be neglected compared to the other sources of uncertainty.

The non-negligible contributions to the polarization value uncertainties are summarized in Table I.

TABLE I. Summary of the individual uncertainties contributing to the total uncertainty of the beam polarization and the Møller electrons polarization in configuration A (values in configuration B are given in parentheses).

	Beam polarization		Møller electrons polarization	
Analyzing power[a]	0.034	(0.033)	0.024	(0.018)
Cuts	0.010	(0.010)	0.010	(0.010)
Beam position	⋯	(⋯)	0.013	(0.013)
Scattering off the collimators[a]	0.019	(0.018)	0.007	(0.006)
False asymmetry[a]	⋯	(0.021)	⋯	(0.006)
Total systematic	**0.040**	(**0.044**)	**0.030**	(**0.026**)
Statistical	0.013	(0.017)	0.022	(0.026)
Total	**0.042**	(**0.047**)	**0.037**	(**0.037**)

[a]Partly cancels out in the polarization ratio.

TABLE II. Results of the beam polarization measurements. $N_L^{\rm beam}$ and $N_R^{\rm beam}$ are the numbers of events (after background subtraction and dead time correction) recorded in the L and R detector, respectively. Single-counter asymmetry values $A_L^{\rm beam}$ and $A_R^{\rm beam}$ were obtained from Eq. (2) and the combined value $A^{\rm beam}$ from Eq. (3). The beam polarization $P^{\rm beam}$ was calculated from $A^{\rm beam}$ and the Monte Carlo value of the effective analyzing power.

	Configuration A	Configuration B
$N_L^{\rm beam}$	$(586.9 \pm 1.3)10^3$	$(561.2 \pm 1.2)10^3$
$N_R^{\rm beam}$	$(653.4 \pm 1.4)10^3$	$(671.9 \pm 1.3)10^3$
$A_L^{\rm beam}$	0.0694 ± 0.0023	0.0482 ± 0.0021
$A_R^{\rm beam}$	0.0748 ± 0.0021	0.0508 ± 0.0019
$A^{\rm beam}$	0.0721 ± 0.0011	0.0495 ± 0.0010
$P^{\rm beam}$	0.851 ± 0.042	0.826 ± 0.047

TABLE III. Results of the Møller polarization measurements. $N_L^{\rm Møller}$ and $N_R^{\rm Møller}$ are the numbers of events (after background subtraction, dead time correction and event selection) recorded in the L and R detector, respectively. Single-counter asymmetry values $A_L^{\rm Møller}$ and $A_R^{\rm Møller}$ were obtained from Eq. (2) and the combined value $A^{\rm Møller}$ from Eq. (3). The Møller electrons polarization $P^{\rm Møller}$ was calculated from $A^{\rm Møller}$ and the Monte Carlo value of the effective analyzing power.

	Configuration A	Configuration B
$N_L^{\rm Møller}$	$(160.19 \pm 0.69)10^3$	$(166.48 \pm 0.57)10^3$
$N_R^{\rm Møller}$	$(210.12 \pm 0.69)10^3$	$(227.63 \pm 0.70)10^3$
$A_L^{\rm Møller}$	0.0291 ± 0.0043	0.0190 ± 0.0034
$A_R^{\rm Møller}$	0.0309 ± 0.0033	0.0133 ± 0.0031
$A^{\rm Møller}$	0.0300 ± 0.0019	0.0161 ± 0.0016
$P^{\rm Møller}$	0.339 ± 0.037	0.258 ± 0.037

VI. RESULTS

A. Beam polarization

The beam polarization values were calculated using Eqs. (3) and (4) from the measured numbers of events and simulated effective Sherman function. The results are listed in Table II. The Monte Carlo value of the effective Sherman function is $S^{\rm beam} = 0.0847 \pm 0.0034$. The energy loss of electrons in the gold target was taken into account in the computations. The effect is approximately 0.1 MeV on average, since the 9.9 μm gold target is relatively thick for electron energies around 3 MeV. In order to calculate the effective Sherman function corresponding to the event selection, Gaussian smearing, reflecting the detector resolution, was applied to the Monte Carlo-generated energy values, and the effective Sherman function was calculated for events selected from the same part of the spectrum as in the data analysis. According to the Monte Carlo simulation, the change of beam polarization in Mott scattering off beryllium at an angle of 26.75° is negligible (below 0.1%).

The beam polarization was independently measured with the MAMI Mott polarimeter [23] operating directly on the beam, yielding 0.835 ± 0.020 and 0.806 ± 0.020, during the data acquisition periods in configurations A and B, respectively.

Both results can be compared in order to verify the correctness of the measurement, as well as the accuracy of the Monte Carlo predictions for the analyzing power. The results are in agreement within 1σ.

B. Møller electrons polarization

The mean polarization values of Møller electrons were calculated using Eqs. (3) and (4) from the measured numbers of events, assuming the Monte Carlo value of the effective Sherman function $S^{\rm Møller} = 0.0886 \pm 0.0063$. The results listed in Table III were obtained by counting events in the full Møller peak (using the $\pm 2\sigma$ energy cuts marked in Fig. 7).

C. Polarization transfer

Since the theoretical predictions refer to the polarization transfer, it is optimal from the uncertainty point of view to determine the ratio of polarizations before and after the scattering. In this case, a large part of systematic errors is strongly suppressed compared to an absolute polarization measurement, since their contributions to both polarization values are of the same nature. This applies, in particular, to the systematic uncertainty of the Monte Carlo predictions and target thickness, which affect the effective Sherman function values at 1.5 and 3 MeV in a similar way.

The measurement results ($P^{\rm Møller}/P^{\rm beam}$, cf. Tables II and III) can be compared to the predicted ratio of polarizations in the initial and final states of Møller scattering, see Table IV. While for configuration A excellent agreement between the experimental value and the theoretical predictions is found, the result in configuration B is about 1.5σ smaller than expected.

In both experimental configurations, Møller scattering took place in the horizontal plane, and the beam polarization was either horizontal or vertical. It allows us to verify the dependence of the polarization transfer on the angle between the beam polarization vector and the Møller

TABLE IV. Polarization transfer (length of the transverse polarization vector component in the final state of symmetric Møller scattering divided by the initial beam polarization). Experimental results are compared to the theoretical predictions [14].

	Configuration A	Configuration B
Experiment	0.398 ± 0.046	0.312 ± 0.046
Theory	0.399	0.382

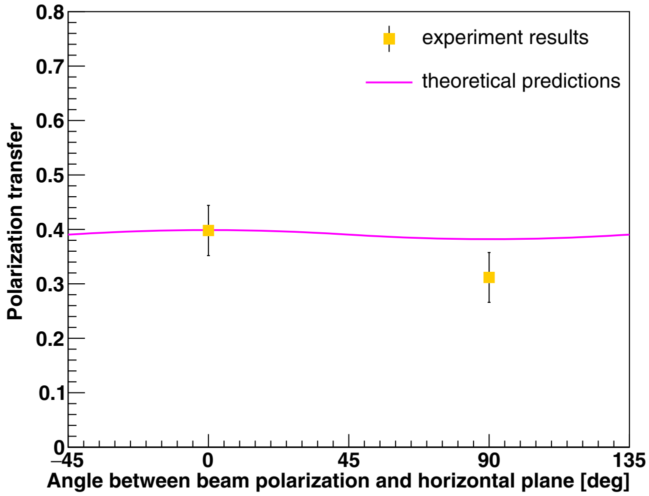

FIG. 8. Polarization transfer (length of the transverse polarization vector component in the final state of symmetric Møller scattering divided by the initial beam polarization), plotted as a function of the angle between the beam polarization vector and the Møller scattering (horizontal) plane. Solid line, theoretical predictions [14]; points, experimental data.

scattering plane, shown in Fig. 8. One can see that the experimental points are in agreement with the predicted theoretical dependence within the present experimental uncertainty. Whether or not the small difference between the experimental and theoretical results for configuration B reflects some real discrepancy can only be assessed in a measurement with increased precision.

VII. PREDICTIONS FOR SPIN CORRELATION MEASUREMENTS

The results of the present measurement allow us to make estimates for a spin-correlation measurement, in which the spin projections of both electrons in the final state have to be measured simultaneously. The number of events recorded in the present experiment, cf. Table III, corresponds to the joint interaction probability of one Møller and one Mott scattering of $p_{\mathrm{exp}} = 7.2 \times 10^{-12}$. The Mott scattering probability of the second electron estimated with the Monte Carlo simulation is $p_{\mathrm{Mott}} \approx 2 \times 10^{-4}$. The number of signal events recorded in a correlation experiment would be lower by the factor p_{Mott}, resulting in a much smaller signal-to-background ratio, necessitating to substantially reduce the background.

In the limiting case of no external background, the signal events probability would be $p_{\mathrm{exp}} p_{\mathrm{Mott}} \approx 10^{-15}$, and the background probability due to false coincidences originating from two different beam electrons would be $p_{\mathrm{exp}}^2 I \Delta t$, where I is the number of beam electrons per unit time (proportional to the beam current) and Δt is the time coincidence window (2 ns in the present case). Taking this into account, the time necessary to measure the spin-correlation probability with 10% relative uncertainty is about 15 days if the measurement is performed at the highest beam current available at MAMI of 20 μA. At such a high current there would be, however, about 20% pile-up events, in which the signals from two electrons overlap.

In reality the fraction of pile-up events will be higher; therefore, a reasonable beam current could be of the order of 1 μA, corresponding to a few percent of pile-up events and the measurement time below one year.

The background level that would be observed in a spin-correlation experiment performed with the present prototype detector was also determined. At the high beam current necessary for the measurement, the statistical uncertainty would be dominated by the number of background events. Assuming that the background rate is proportional to the square of the beam current, one can calculate the background event probability corresponding to a given statistical uncertainty and measurement time. The background must be reduced by about 4 orders of magnitude in order to measure the correlation probability with a relative uncertainty of 10% within a reasonable beam time of the order of one year.

Several improvements of the experimental setup are possible to reduce the background rate. The Mott polarimeters could be equipped with additional tracking detectors placed in the polarimeter arms, in coincidence with the existing ones, and the arms can be surrounded with veto detectors, read out in anticoincidence, both of which would reduce the rate of external background. Faster detectors would reduce the rate of false coincidences as well as the fraction of pile-up events. In light of the very low cross sections, such a measurement might also require a further increase of the collimator aperture in the Mott polarimeter. In addition, the cross sections could be increased by reducing the incident-beam energy. The experiment can also be performed with more than one Møller or Mott scattering plane, allowing us to collect data in several configurations simultaneously.

VIII. SUMMARY AND CONCLUSIONS

Møller electrons backscattered off a gold target were observed in a Mott polarimeter and efficiently distinguished from the background. The asymmetry of the polarimeter count rates arising from the beam polarization was measured. The beam polarization, as well as the mean polarization of the electrons in the final state of symmetric Møller scattering, was calculated assuming a Monte Carlo value of the analyzing power.

The beam-polarization value was found in good agreement with an independent direct measurement, which confirmed the correct operation of the polarimeter. The ratio of polarizations before and after Møller scattering was compared to the predictions of relativistic quantum mechanics. The measurements were performed in two experimental configurations corresponding to two orientations of the beam polarization, and both results are in agreement with the theoretical predictions.

Our measurement demonstrates that a standard Mott polarimeter is a suitable tool for measuring polarization with a divergent stream of Møller electrons despite the high-background environment.

While the measurement of the mean polarization allows the average spin state of individual electrons to be investigated, the measurement of spin correlations can give insight into the phenomenon of entanglement in relativistic Møller scattering. Such a measurement would be much more challenging; however, several improvements towards an optimized experimental setup are possible.

ACKNOWLEDGMENTS

We would like to thank Prof. K. Aulenbacher and Prof. A. F. Żarnecki for helpful discussions. We are also indebted to T. Eggert, M. Herbert, M. Meier, and M. Peck for assistance during the data acquisition. This work was supported by National Science Centre Grant No. 2017/25/N/ST2/00619 (M. Drągowski), by the German Academic Exchange Service (DAAD), and through DFG Research Training Group 2128 “AccelencE” (Project No. 264883531).

[1] Ch. Møller, Ann. Phys. (N.Y.) **14**, 531 (1932).
[2] Ya. B. Zeldovich, J. Exp. Theor. Phys. **36**, 964 (1959).
[3] P. L. Anthony *et al.*, Phys. Rev. Lett. **95**, 081601 (2005).
[4] P. S. Cooper *et al.*, Phys. Rev. Lett. **34**, 1589 (1975).
[5] K. Aulenbacher, E. Chudakov, D. Gaskell, J. Grames, and K. D. Paschke, Int. J. Mod. Phys. E **27**, 1830004 (2018).
[6] J. M. Grames *et al.*, Phys. Rev. ST Accel. Beams **7**, 042802 (2004).
[7] T. J. Gay and F. B. Dunning, Rev. Sci. Instrum. **63**, 1635 (1992).
[8] A. Einstein, B. Podolsky, and N. Rosen, Phys. Rev. **47**, 777 (1935).
[9] J. S. Bell, Physics **1**, 195 (1964).
[10] M. Lamehi–Rachti and W. Mittig, Phys. Rev. D **14**, 2543 (1976).
[11] S. Hamieh *et al.*, J. Phys. G **30**, 481 (2004).
[12] H. Sakai *et al.*, Phys. Rev. Lett. **97**, 150405 (2006).
[13] P. Caban, J. Rembieliński, and M. Włodarczyk, Phys. Rev. A **88**, 032116 (2013).
[14] M. Włodarczyk, P. Caban, J. Ciborowski, M. Drągowski, and J. Rembieliński, Phys. Rev. A **95**, 022103 (2017).
[15] K. Bodek, P. Caban, J. Ciborowski, J. Enders, A. Köhler, A. Kozela, J. Rembieliński, D. Rozpędzik, M. Włodarczyk, and J. Zejma, AIP Conf. Proc. **1563**, 208 (2013).
[16] J. Kessler, *Polarized Electrons*, 2nd ed. (Springer, Berlin, 1985).
[17] G. D. Fletcher, T. J. Gay, and M. S. Lubell, Phys. Rev. A **34**, 911 (1986).
[18] F. Salvat, A. Jablonski, and C. J. Powell, Comput. Phys. Commun. **165**, 157 (2005).
[19] S. Agostinelli *et al.*, Nucl. Instrum. Methods Phys. Res., Sect. A **506**, 250 (2003).
[20] M. Drągowski, M. Adamus, G. Weber, and M. Włodarczyk, Nucl. Instrum. Methods Phys. Res., Sect. B **488**, 37 (2021).
[21] A. Jankowiak, Eur. Phys. J. A **28**, 149 (2006).
[22] S. Ritt, *2008 IEEE Nuclear Science Symposium Conference Record, 1512–1515* (IEEE 2008).
[23] V. Tioukine, K. Aulenbacher, and E. Riehn, Rev. Sci. Instrum. **82**, 033303 (2011).
[24] M. Drągowski *et al.*, Monte Carlo Simulation of the Effective Sherman Function for Electron Polarimetry in the MeV Energy Range (to be published).
[25] X. Roca-Maza, Europhys. Lett. **120**, 33002 (2017).
[26] Y. S. Tsai, Phys. Rev. **120**, 269 (1960).